Title

High expression of CAI2, a 9p21-embedded long noncoding RNA, contributes to advanced-stage neuroblastoma.

Journal

Cancer research, 74(14)

ISSN

1538-7445

Authors

Barnhill, Lisa M
Williams, Richard T
Cohen, Olga
et al.

Publication Date

2014-07-15

Peer reviewed

High expression of CAI2, a 9p21-embedded long non-coding RNA, contributes to advanced stage neuroblastoma.

Running title: A 9p21 localized lncRNA associated with neuroblastoma

Authors:

Lisa M. Barnhill[1], Richard T. Williams[1], Olga Cohen[1], Youngjin Kim[1], Ayse Batova[1], Jenna A. Mielke[1], Karen Messer[2], Minya Pu[2], Lei Bao[2], Alice L.Yu[1, 3, 4], Mitchell B. Diccianni[1]

[1, 6] University of California San Diego, Dept. of Pediatrics Hematology/Oncology, San Diego, CA 92103-8447, tel: 619-543-2436; fax: 619-543-5413

[2] Division of Biostatistics and Bioinformatics, Moores UCSD Cancer Center, La Jolla, CA 92093-0901

[3] Academia Sinica, Genomics Research Center, Taipei 115, Taiwan;

[4] Institute of Stem Cell & Translational Cancer Research, Chang Gung Memorial Hospital at Linkou, Taoyuan, Taiwan

lbarnhil@pointloma.edu, olcohen@ucsd.edu, y32kim@gmail.com, r6williams@ucsd.edu, abatova@ucsd.edu, kmesser@ucsd.edu, mpu@ucsd.edu, lebao@ucsd.edu, aliceyu@ucsd.edu, mdiccianni@ucsd.edu.

Key Words:

lncRNA

CAI2

neuroblastoma

9p21

p16

Funding: Biomarker research in neuroblastoma is supported by grants from the NIH (CA164132 to A.L. Yu), Alex Lemonade Stand Foundation and the Children's Oncology Group.

DNA sequencing was performed by the DNA Sequencing Shared Resource, UCSD Cancer Center, which is funded in part by NCI Cancer Center Support Grant # 2 P30 CA023100-23.

Corresponding Authors: Mitchell B. Diccianni and Alice L Yu, UCSD, Dept. of Pediatrics Hematology/Oncology, 200 W. Arbor Dr, San Diego, CA 92103-8447. mdiccianni@ucsd.edu and aliceyu@ucsd.edu; tel: 619-543-2436; fax: 619-543-5413.

Conflicts of Interest: The University of California San Diego has filed a patent on CAI2 in which MBD, ALY, LB and YK are named as co-inventors.

Abbreviations:

lncRNA; long non-coding RNA
ncRNA; non-coding RNA
CAI2; CDKN2A/ARF Intron 2 non-coding RNA
MNC; Peripheral blood mononuclear cells
RACE; Raid Amplification of cDNA Ends
ORF; Open Reading Frame
AA; Amino Acids
chARF; chimeric ARF
p16-ACT; p16-Alternate Carboxy Terminus
RT; reverse transcriptase
qRT-PCR; quantitative RT-PCR
SRC; Spearman-Rank correlation
HR, hazard ratio
CI, confidence interval
EFS, event-free survival
OS, Overall survival

Abstract:

Neuroblastoma is a pediatric cancer with significant genomic and biological heterogeneity. p16 and ARF, two important tumor suppressor genes on chromosome 9p21, are inactivated commonly in most cancers but paradoxically overexpressed in neuroblastoma. Here we report that exon γ in p16 is also part of an undescribed long non-coding RNA (lncRNA) that we have termed CAI2 (CDKN2A/ARF Intron 2 lncRNA). CAI2 is a single exon gene with a poly A signal located in but independent of the p16/ARF exon 3. CAI2 is expressed at very low levels in normal tissue but is highly expressed in most tumor cell lines with an intact 9p21 locus. Concordant expression of CAI2 with p16 and ARF in normal tissue along with the ability of CAI2 to induce p16 expression suggested that CAI2 may regulate p16 and/or ARF. In neuroblastoma cells transformed by serial passage in vitro, leading to more rapid proliferation, CAI2, p16 and ARF expression all increased dramatically. A similar relationship was also observed in primary neuroblastomas where CAI2 expression was significantly higher in advanced stage neuroblastoma, independently of MYCN amplification. Consistent with its association with high risk disease, CAI2 expression was also significantly associated with poor clinical outcomes, although this effect was reduced when adjusted for MYCN amplification. Taken together, our findings suggested that CAI2 contributes to the paradoxical overexpression of p16 in neuroblastoma, where CAI2 may offer a useful biomarker of high-risk disease.

Introduction:

It is becoming increasingly apparent that long non-coding RNAS (lncRNAs), which until recently were thought to have little functional significance, harbor diverse roles in regulating cell identity, differentiation, and development. They have been implicated in cellular and molecular regulation, with chromatin remodeling and gene regulation emerging as common functions (1). In addition to normal cellular regulatory roles, lncRNAs are often deregulated in a wide variety of diseases (1-4). For example, the lncRNA *CRNDE*, originally identified through its association with colorectal cancer, is elevated in multiple cancer types and is induced during neuronal differentiation (5). One of the most well characterized lncRNAs, the HOX gene antisense lncRNA HOTAIR, has been shown to serve as a tumor biomarker in various types of cancers including breast, esophageal and pancreatic, and has also been correlated with tumor progression and prognosis (6-9).

Initiating from discrete first exons separated by ~20Kb on 9p21, the transcripts of *p16* ($p16^{Ink4a}$) and *ARF* ($p14^{ARF}$) are spliced onto a common exon 2 in separate reading frames and code for two different growth regulatory proteins. In addition, a homologous third tumor suppressor gene, p15 ($p15^{Ink4b}$), lies on 9p21 ~10Kb telomeric of ARF. Given the central role these proteins play in cell cycle regulation, it is not surprising to find that the inactivation of all three have been associated with the pathogenesis of many human cancers (10, 11). Additionally, genome-wide association studies (GWAS) studies also implicate this locus with coronary disease, intracranial aneurysm, and diabetes (for review see (12)), demonstrating that this chromosomal region is a major player in a wide range of diseases. 9p21 is also the home of two lncRNAs, *ANRIL* and *p15AS* (*CDKN2BAS*) (13, 14). Functionally, both act as regulators of growth. *ANRIL* has been shown to regulate its neighbor tumor suppressors *p16* and *ARF* and thereby regulate cell proliferation and senescence (15-17). Expression of exogenous *p15AS* caused *p15* silencing and increased growth through heterochromatin formation and DNA methylation (14).

Neuroblastoma is the third most common malignancy of childhood. Diagnosed in stages based on clinical and biological features, patients with a favorable (low-risk disease) diagnosis can often be cured. However, approximately 50% of patients have high-risk disease and have dismal outcomes despite multi-agent and multi-modality therapy, myeloablative therapy followed by autologous bone marrow transplantation, with more than half of the patients nevertheless relapsing and succumbing to the tumor. Recently, we have reported on the significant improvement in survival targeting the GD2 tumor associated antigen uniformly expressed by

neuroblastoma (18). Nevertheless, approximately one third of the patients continue to fail, highlighting the need to identify biomarkers to better predict outcome and improve efficacy.

While investigating the role of p16 in neuroblastoma, we observed that, in contrast to most tumors, p16 was not inactivated but paradoxically was overexpressed (19). Notably, p16 overexpression was significantly associated with advanced stage disease and a poor outcome (20). Upon continued investigation in neuroblastoma cell lines, we identified a unique transcriptional variant, p16γ, which is formed by the splicing of the cryptic exon gamma, located in p16 intron 2, onto p16 exons 2 and 3 (21). It was our investigations into *p16*γ that led to the discovery we report here that exon γ is also part of a lncRNA we call *CAI2*, a single-exon, intron-localized, polyadenylated gene. *CAI2* is expressed at high levels in many tumor cell lines and its expression is highly correlated with the expression of *p16* and *ARF*. In neuroblastoma, *CAI2* expression was significantly associated with advanced stage disease and a poor outcome, suggesting that CAI2 may be a novel biomarker of neuroblastoma patient risk.

Materials and Methods:

DNA and RNA preparation, *RACE* and amplification:

DNA was isolated using the Gentra DNA isolation kit and total RNA from cell lines extracted using Trizol reagent (Life Technologies). The 5' end of *CAI2* gene was obtained using both the GeneRacer kit (Life Technologies) and the SMART RACE cDNA amplification kit (Clontech) with DNAse-treated total RNA from HeLa cells. RACE products were cloned into pCR4-TOPO vector (Life Technologies) and sequenced. For RT-PCR, DNAse-treated RNA was reverse-transcribed using SuperScript III (SSIII) First-Strand Synthesis System with oligo-dT primers (Life Technologies). Quantitative RT-PCR (qRT-PCR) amplifications were performed on an ABI 7300 Real-Time PCR System using Quantitech SYBR Green Master Mix (Qiagen #204143) or Sybr Select Master Mix (Life Technologies #4472908) and compared to β-actin, or using Life Technologies Taqman assays (p16 – Hs02902543_mH, ARF – Hs99999189_m1, TH – Hs00165941_m1) and compared to GAPDH (Hs99999905_m1). Amplifications were performed in a final volume of 25 µL with an initial incubation at 50°C for 2 min followed by one cycle of denaturation (95°C for 10 min). Sybr green amplifications utilized 40 amplification cycles of 30 sec each at 95°C, 60°C and 72°C followed by a dissociation step, while Taqman utilized 45 cycles of 95°C for 15 sec and 60°C for 1 min. Each sample was amplified in duplicate and each experiment performed at least twice. Expression was determined from the qRT-PCR data and analyzed using the $2^{-\Delta\Delta Ct}$ algorithm.

Primers:

BS-ACT, 5'-GAAACTACCTTCAACTCCATC-3';
BR-ACT, 5'-GTAGAAGCATTTGCGGTGGACGATGGAGGGGCC-3';
p16S, 5'-CTGGAATTCAGCATGGAGCCGGCGGCGGGGAG-3';
c359R, 5'-GCGCGCAGGTACCGTGC-3';
c257F, 5'-TCGTGCTGATGCTACTGAGG-3';
I2796R, 5'-GAAGGCGTGAAGATGTGG-3';
Gam517F, 5'-GTGGGTTTGTAGAAGCAGGC-3';
ARF-SYR, 5'-CCATCATCATGACCTGGTCTTCT-3';
I1698F-Bam, 5'-CAATTAGAGCGCGGATCCAGGG-3';
3p16, 5'-CTACGAAAGCGGGGTGGGTTGT-3';
1888F-Bam, 5'-ATCGGGATCCAACCCCCTCTTCAAGCACAAT-3'
2252R-Xho, 5'-ATCGCTCGAGAAGGGCAAGATAGCTTGGGACT-3'
TH-666F, 5'CTGACCTGGACTTGGACCAC-3'

Th-763R, 5'-GTCGCCGTGCCTGTACTG-3'

Primers (at 10 μM unless indicated) used for qRT-PCR: *p16*: p16S-Eco & c359R (13.5 μM each); *CAI2*: GAM517F (13.5 μM) & I2796R (4.5 μM); *ARF*, c257F & c359 or ARF-SYR; *β-actin*: BS-ACT and BR-ACT; TH: TH-666F and TH-763R.

Expression Constructs:

Full-length *p16* (pcp16) (21) and *CAI2* (pc*CAI2)* expression constructs were constructed in pcDNA3.1 (Invitrogen); *CAI2* (ps*CAI2*) was also created in pSilencer4.1-CMV vector (Ambion). *CAI2* was cloned from an amplicon generated with primers I1698 and 3p16. All constructs were sequence and expression validated, with *p16* further validated by Western blot.

For reticulocyte assay, we used full length pcp16 or *CAI2* and ORF2 (amplicon from primer set 1888F and 2252R) cloned into pCR2.1-TOPO (Invitrogen) in both the sense (*CAI2* and ORF2) and antisense (*CAI2*) directions. All constructs were sequence validated and protein production assessed with the Promega TNT Coupled Reticulocyte Lysate System using ^{35}S-Methionine and ^{35}S-Cysteine.

Tissue, Cell Lines, Cell Culture, Cell Growth and Transfections:

Normal human tissue RNA was from Clontech. FS15 are low passage cultures of foreskin fibroblasts generously provided by Dr. Bruce Barshop (UCSD). The source of the cell lines and culture conditions has been documented previously (19, 22). Cells were transfected at 70-90% confluence using Lipofectamine 2000 reagent (Invitrogen) or with the NEON electroporation apparatus (Invitrogen). Post-transfection incubations proceeded for 24h to 72h, after which cells were observed, counted, assayed and/or harvested as appropriate. Primary sample and cell line RNA was isolated using Trizol (Invitrogen). All RNA samples were subjected to DNAse treatment and repurification using the Zymo Research RNA Clean & Concentrator kit.

Primary Tumor Samples:

A total of 62 samples of primary neuroblastoma tumors with a tumor cell content of ≥80% were obtained from the Children's Oncology Group. The patients had an average age of diagnosis of 1.6 years (range 0 -12.2 years), with an average follow-up of those who have had no event (relapse or death) of 3.8 years (range 0.8 -9.5 years). Samples distributed as follows: 10 stage 4S, 11 stage 1, 12 stage 2, 9 stage 3 and 20 stage 4. The clinical stages were classified as favorable stage/low risk (stages 1, 2, and 4S), unfavorable stage/moderate risk (stage 3) or unfavorable stage/high risk (stage 4) based on COG staging criteria. Tumor samples were collected after informed consent and used under an UCSD approved IRB.

NMB7 cells:

For the serial passage experiments, a fresh thaw of low passage NMB7 was plated in complete media and, at the passage indicated, cells were released from the plate with trypsin, and a portion of the cells lysed in Trizol for RNA extraction while a separate portion was reseeded for continued growth. The serial passage experiments were done twice, while RNA extractions from low and high passage cultures were done multiple times. For treatment comparisons, NMB7 cells at passage 5 or passage 16 were plated in 6 well plates at 125,000 cells in 10% FBS supplemented RPMI with antibiotics. After an attachment period, the media was removed and replaced with fresh media either without serum, with serum plus 0.5% DMSO or with serum plus 5 μM RA (Sigma R2625 with 0.5% DMSO final concentration) and cells allowed to grow for an additional 24h or 72h, after which they were evaluated and, in some experiments, lysed in Trizol. Cells were photographed in independent experiments either directly or after H&E staining at 40X under phase-contrast. For growth experiments, 50,000 low or high passage cells were plated, allowed 24h to adhere, then observed and counted at 24h intervals up to 96h. Doubling time (DT) was calculated as DT=h*ln(2)/ln(c2/c1)), where h is time in hours and C1 and C2 are the beginning and ending number of cells present.

Statistical analysis:

A Spearman's Rank Correlation (SRC) was used to analyze assess correlations between in expression data and a continuous outcome, a Kruskal-Wallis test used to test the association between CAI2 expression and a categorical variable such as stage, and a Wilcoxon Rank sum test used to test the association between CAI2 expression and a binary variable such as MYCN status. A logrank test was used to assess the association a survival outcome and a binary predictor, and a Cox model was used to assess these associations adjusted for other covariates such as age at diagnosis. Anova was used to compare expression across multiple parameter or time points, with individual analyses compared by t-test. P values less than 0.05 were considered statistically significant.

Results:

I. Discovery of CAI2 (CDKN2A /ARF/ Intron 2 non-coding RNA) by RACE

While exploring *p16γ* expression, we observed that the gamma exon was present in many more samples than in which *p16γ* could be detected. Speculating that the gamma exon may be part of another alternatively spliced transcript of *p16*, we employed RACE (Rapid Amplification of cDNA Ends) to explore potential novel 5' ends using DNase-treated total RNA from HeLa cells. The 5' RACE amplification product using the Invitrogen GeneRacer kit resulted in a sharp band and a uniform smear of increasing molecular weight (Fig 1A). Sequence analysis of the extracted, purified and cloned RACE products revealed the sharp RACE band encompassed not only exon γ, but extended upstream to 1256 bases from the 3' end of p16 exon 2 (Fig 1B). Sequence analysis of the smear yielded identical sequence except contained a concatemer of the RNA oligonucleotide adapter on the 5' end. A second RACE analysis using the DNA-oligo adaptor method (Clontech) also yielded a single amplicon, which subcloning and sequence characterization revealed a 5' end that was within 30 bases of the transcript characterized using the GeneRacer kit and a 3' end that terminated 226 bases after the p16 stop codon (Fig 1B). Amplifications with sense primers to exon 2, exon 1α or exon 1β yielded amplicons with p16 3'-UTR primers but not with *RACE*-region antisense primers. On the other hand, *RACE*-region sense primers easily amplified with the 3'-UTR primers (data not shown). Furthermore, transcript amplification could only be demonstrated from RNA subjected to the RT reaction (Fig 1E). Taken together, this data demonstrates that this intronless transcript is not DNA contamination and is independent of p16 and ARF.

II. CAI2 is a non-conserved non-coding RNA

A bioinformatic analysis of this transcript revealed 5 open reading frames (ORF) with a length of 40 amino acids or greater (Fig 1C). The largest, ORF2, predicts a putative protein of 107 residues that a cross-species comparative analysis revealed only weak homologies (≤57%) that were limited to upper primates, consistent with the presence of an Alu element in this region. A comprehensive comparative analysis of the entire *CAI2* nucleotide sequence also revealed no significant homologies with the exception of the expected p16 exon 3 and the Alu region of ORF2. We nevertheless assessed possible translation using the TNT Reticulocyte Lysate System (Promega Corp). However, no evidence of a protein was observed from the transcript oriented in either direction nor ORF2 in the sense direction (Fig 1D). These experiments revealed the gamma exon is part of an uninterrupted 1643 base non-coding

transcript we call *CAI2* (*CDKN2A/ARF* Intron 2 lncRNA) that is distinct from *p16, ARF* and *p16γ* (Fig 1B). The complete sequence is presented in Supplemental Table S1.

III. Expression of CAI2 in relation to the p16 and ARF

We compared the expression profile of *CAI2* in 46 tumor cell lines and 5 non-tumor samples, with representative amplifications shown in Fig 1F and summarized in Supplemental Table S2. The expression profiles of *p16, ARF* and *CAI2* were similar in most cell lines, where 20 of 26 cell lines with an intact 9p21 locus expressed all three genes robustly. Of the remaining six, all expressed *ARF* high and *p16* low while expression of *CAI2* was mixed. In contrast to tumor cell lines, none of the five non-tumor samples appreciably expressed *CAI2*. Considering whether this was a general characteristic of non-neoplastic cells, we undertook a quantitative assessment of *CAI2* expression in 25 normal samples. When each gene was normalized and graphed individually against expression in fibroblasts, most tissues exhibited similar levels of expression (>0.5 to <5.0 fold), with expression much lower (<0.5 of control) in just six and very high in two (spinal cord and adrenal). In contrast, p16 and ARF expression were much lower than fibroblasts in most tissues (Supplemental Figure S1). However, normalizing each gene to itself hides fact that CAI2 expression is much lower than that of p16 and ARF in many tissues, including fibroblasts. As illustrated in Figure 2A, when all three genes were normalized to CAI2 in fibroblasts, the low expression of *CAI2* in comparison to p16 and ARF was almost ubiquitous with the exception of spinal cord, which expressed *CAI2* ~200-fold higher than normal fibroblasts, and adrenal gland at ~16-fold higher. In contrast, other tissues tested expressed *CAI2* at levels similar to or much lower than fibroblasts, with the lowest levels (~0.1-fold) seen in fetal tissue, kidney and heart. *P16* and *ARF* are independent genes with independent promoters that share correlated expression profiles. Consistent with this, a Spearman Rank Correlation (SRC) analysis of *ARF* and *p16* expression showed a significant association (SRC = 0.68, $p<0.001$), with an even stronger correlation *of CAI2* with both genes (*p16* SRC = 0.73, $p<0.0001$; *ARF* SRC = 0.89, $p<0.0001$) (Figure 2B). We hypothesized that CAI2 could be a regulator of p16 and/or ARF. No neuroblastoma cell line was low for all three genes, though NMB7, IMR32 and PCL1643 were low for both CAI2 and p16 (Supplemental Table S2). Using the NMB7 cell line, which unlike the other two cell lines grow rapidly, as dispersed cell populations and are easily transfected (Fig 2C), we overexpressed CAI2 and observed a small induction of both *p16* and *ARF* expression (2-7 fold), consistent with this hypothesis, though the lack of an influence on cell growth (Fig 2D) suggests that the levels of induction may be too small to be functionally significant.

IV. CAI2 and neuroblastoma cell line transformation

The ability to be induced to differentiate is a characteristic of many neuroblastoma cell lines. We observed that NMB7 cells, with serial passage and without additional treatment, morphologically change from cells with a rounded, trapezoidal morphology (Fig 3A) to a thinner, more elongated phenotype with long processes (Fig 3B). Tyrosine Hydroxylase (TH) expression is known to increase as neuroblastoma cells differentiate (23). However, with increasing passage number, *TH* expression *decreased* by more than 100-fold (Fig 3C, $p<0.001$, Anova), suggesting that the morphological change did not represent a normal differentiated phenotype. The NMB7 cell line at low passage number is also one of the few neuroblastoma cell lines that does not appreciably express *CAI2* (Supplemental Table S2). However, with serial passage, *CAI2*, *p16* and *ARF* expression each exhibited greater than 100-fold increases in expression (Fig 3C, $p<0.001$ for CAI2 and ARF, $p<0.01$ for p16, Anova). And counter to the growth suppressor effects expected of p16 and ARF, high passage cells proliferated more rapidly than low passage cells, with a doubling time of 22h vs. 29h (Supplemental Figure S2).

Retinoic acid (RA) can induce differentiation and death in neuroblastoma cell lines. Treatment of low passage NMB7 cells with 5 μM RA resulted in a visible loss of viability within 24h, with more than 95% of the cells having detached by 72h, while high passage NMB7 cells showed no effect from the RA treatment (Supplemental Table S3). The 24h RA treatment had no significant effect on TH, ARF or p16 gene expression in the high or low passage cell lines, though *CAI2* expression decreased in the low passage cell line (0.39-fold, $p=0.02$, t-test, Fig 3D). Serum deprivation can also induce neuroblastoma cell line differentiation. Serum starved low passage NMB7 showed visible morphological signs of stress with cells looking “stringy” by 24h, rounded by 48h (Supplemental Figure S3) and detached by 72h; *TH* expression increased moderately within 24h of serum starvation (8.8-fold, $p=0.05$, t-test, Fig 3D), an indication differentiation was beginning. On the other hand, there were no significant changes in the expression of *CAI2, p16* or *ARF* ($p>0.05$, Anova). In contrast high passage NMB7 cells showed no negative effects from serum starvation, with no visible morphological changes or changes in the (already elevated) expressions of CAI2, p16 or ARF (Fig 3D and Supplemental Figure S3).

V. Enhanced mRNA levels of CAI2 in advanced stage neuroblastoma.

As most neuroblastoma cell lines are derived from advanced stage tumors with high risk disease (24), and many of the neuroblastoma cell lines highly expressed *CAI2* (Supplemental Table S2), we considered whether this represented a unique feature of cell lines or reflected a characteristic of advanced stage tumor. An examination using RNA from primary neuroblastoma tumors revealed that the 33 prognostically favorable tumors (stages 4s, 1 and 2) expressed low

levels of *CAI2* that were similar to that found in most normal tissues, though an occasional very high expressor was noted (Figure 4A). In comparison, the 29 high risk/stage 4 neuroblastoma expressed significantly higher levels of *CAI2* than favorable outcome group (Figure 4A, p=0.005, Kruskal-Wallis test comparing stage 4s, 1 and 2 vs. stage 3 vs. stage 4). Interestingly. a significant trend could be established when comparing lowest stage to highest stage neuroblastoma (SRC = 0.33, p=0.01), though expression was not significantly associated with MYCN amplification status (Wilcoxon Rank sum test, p=0.18, n= 62 patients at all stages; p=0.88, n=29 stage 3 and 4 patients only). CAI2 expression was also significantly associated with age at diagnosis (SRC=0.39, p<0.002, Figure 4B). Age over the age of 1 year is a negative prognostic factor in neuroblastoma, and most of the patients with high levels of CAI2 delineated to the high risk category. Thus we were concerned that an association with age could be an artifact of prognostic features. However, when we limited the analysis to only high risk stage 3 and 4 patients, CAI2 expression remained significantly associated with age of diagnosis ((SRC=0.38, p<0.05, Figure 4C).

We next considered survival outcomes, with the three patients who had no follow up data censored at day 0, and dichotomized CAI2 expression at 35.9, which was the median of CAI2 values from the stage 3 and 4 patients, resulting in a “high CAI2 expression” population that was comprised of 4 out of 33 stages 1, 2, and 4s patients, 2 out of 9 stage 3 patients, and 13 out of 20 stage 4 patients (Figure 4A). Among all patients, higher CAI2 expression was significantly associated with shorter event-free survival (hazard ratio (HR) for higher vs. lower CAI2 expression = 2.88, 95% confidence interval (CI) = (1.12, 7.45), logrank test p=0.022, Figure 5A) and showed a significant association with overall survival (HR = 3.27, 95% CI = (1.1, 9.77), logrank test p=0.025, Figure 5B). However, when we limited our analysis to only stage 3 and 4 patients, the association of CAI2 expression with either EFS or OS was no longer apparent (HR=1.84 and p=0.26 for EFS, Figure 5C, and HR=1.37 and p=0.58 for OS, Figure 5D). Thus CAI2 expression, in this limited data set, was a prognostic factor associated with a poor outcome, but by itself did not predict survival.

MYCN amplification is a very strong prognostic factor in neuroblastoma. Therefore, we wanted to determine if CAI2 expression added prognostic information over and above MYCN amplification status, using Cox proportional hazards regression models which contained both factors. As expected, MYCN amplification status was a strong negative prognostic factor for both EFS and OS, and remained so even when CAI2 expression was added to the model. On the other hand, the association previously observed between higher CAI2 expression and

outcome was attenuated in the model containing both factors in the entire population for both EFS (adjusted HR for higher vs. lower CAI2 expression = 2.19, 95% CI = (0.81, 5.94), p=0.12) and OS (adjusted HR = 2.39, 95% CI = (0.76, 7.52), p=0.14). Similarly, when we limited the analysis to the stage 3 and 4 population only in the model containing both factors, the association of CAI2 expression with either EFS or OS remained unapparent (HR=1.67, 95% CI = (0.56, 4.97), p=0.36 for EFS, or HR=1.25, 95% CI = (0.40, 3.88), p=0.70 for OS).

Discussion:

The hallmark of neuroblastoma is its clinical and biological heterogeneity, with treatment based on subgroups defined by age at diagnosis, extent of disease and tumor biology. Clinically, risk stratification has been very successful. However, it remains true that some patients with identical risk factors who receive the same treatment can have considerably different outcomes. For example, though immunotherapy with ch14.18 has resulted in significant decreases in relapse and a significant improvement in cure rate, almost one-third of the children continue to fail therapy and succumb to the disease (18). The challenge, therefore, is to refine risk stratification through the identification of biomarkers and novel biological targets.

The over- and under-expression of ncRNAs have been associated with neuroblastoma prognosis. We and others have shown that microRNA (miRNA) expression profiles can differentially identify high versus low risk neuroblastoma (25, 26). The lncRNA lncRAN is overexpressed and prognostically significant in neuroblastoma and bladder cancer (27, 28). In a bladder cancer cell line, overexpression of lncRAN enhanced the proliferation, migration, and invasion of the cells, while its suppression enhanced chemosensitivity (28). Expression of the ncRNA *NDM29* correlated with growth rate of neuroblastoma and other tumor cell lines in an inverse fashion, with low expression correlating with a faster growth while overexpression in the SKNBE2 neuroblastoma cell line led to their differentiation and an increased chemosensitivity (29). The diverse family of genes known as transcribed ultra-conserved regions (T-UCRs) are another class lncRNAs of that have been implicated in neuroblastoma through their association with MYCN amplification, outcome of high risk/stage 4 patients and RA response (30-32). Many of the characteristics of *lncRAN*, *NDM29* and the T-UCRs are similar to what we find with *CAI2* in neuroblastoma. In NMB7, cellular “transformation” is accompanied by not only an increase in *CAI2* expression, but a loss of sensitivity to RA. High passage NMB7 cells also express significantly higher levels of CAI2 and proliferate faster than low passage NMB7 cells. CAI2 was also expressed highly in most tumor cell lines but low in normal cells, suggesting a possible correlation with growth rate.

9p21 is a chromosomal region implicated in many different cancers, with deletion/mutation/epigenetic inactivation of p16 and ARF almost universal events in cancer. However, neuroblastoma has been a glaring exception. In fact, it has been more than a decade since we first reported on the paradoxical overexpression of *p16* in advanced stage neuroblastoma and its association with poor outcome (20). As ncRNAs play regulatory roles, aberrant expression of these molecules may contribute to the paradoxical p16 expression. We

considered mir-24, a regulator of p16 (33). However, we and others have not observed this microRNA to be differentially expressed in neuroblastoma (25, 26). ANRIL has also been shown to negatively regulate p16 expression (15, 16), though the expression status of ANRIL in neuroblastoma remains unknown. With the discovery that CAI2 can modulate *p16* and *ARF* expression *in vitro,* there is now an alternative pathway of p16 regulation to consider. A role in neuroblastoma is also supported by our findings that CAI2 is overexpressed in advanced stage neuroblastoma and is an independent prognostic factor.

Despite strong associations, we did not see an effect of CAI2 on NMB7 cell growth, either negative or positive, after transient transfections, and the effect on p16 was only minimal. It is possible that the conditions we are evaluating the effect of CAI2 on growth and p16 expression are inappropriate. For example, if CAI2 optimally influences p16 expression under conditions of stress or DNA damage response, p16 levels may not appreciable change when CAI2 is overexpressed in normal, proliferating cell lines. This would be similar to the actions performed by ANRIL, which suppresses p16 and ARF expression in response to DNA damage (16). The observation that the highest levels of CAI2 are seen in spinal cord, a conduit of stress response, supports this idea. Alternatively, if CAI2 is a transcript “stabilizer” like the lncRNA BASE1-AS (34), then overexpression might again only exhibit a minimal effect. Several lncRNAs have been shown to transcriptionally regulate indirectly through epigenetic actions. For example, the recently reported lncRNA ecCEBPA is a regulator of DNA methylation (35) while HOTAIR and ANRIL bind and modulate the Polycomb-repressive complex (36), which is required for epigenetic silencing during development and cancer. However, we showed many years ago that p16 is not methylated in neuroblastoma (19, 22), perhaps precluding the observation of a significant influence of CAI2 on p16 expression.

The fact that CAI2 has only a marginal impact on its nearest neighbor genes while seeming to have a considerable impact on tumor cell growth and survival, as evidenced by its preferential expression in advanced stage neuroblastoma and association with outcome, may suggest that CAI2 acts in a more global manner and the regulation of p16 and/or ARF are not its primary functions. The NMB7 cells during “transformation” undergo a significant change in morphology, growth, and drug sensitivity consistent with advanced stages of neuroblastoma. The inappropriate overexpression of CAI2 may at least facilitate such a “reprogramming”. The possibility of a more global function would be consistent with the histone modification actions of HOTAIR and ANRIL (37). Studies have shown lncRNAs play roles in multiple biological processes, including dosage compensation, genomic imprinting, chromatin remodeling, alternative splicing and nuclear organization (38). A recent study has also shown actions on

proliferation, apoptosis, metastasis and autophagy (39). Exploring possible binding partners of CAI2 will give insight into pathways associated with the gene and clues to its function, as will its overexpression and/or silencing in moderate p16/ARF/CAI2 expressing model systems.

In summary, it is clearer than ever that the 9p21 locus, which is undoubtedly important in cancer, represents a complicated locus. It harbors three tumor suppressor genes *p16*, *ARF*, *p15*, the alternative spliced *p16*γ (21) and *p10* (40), the contiguously transcribed *p12* (41), mutation generated hybrid proteins such as chimeric ARF (chARF) and p16-Alternate Carboxy Terminus (p16–ACT) (42), the metabolic gene MTAP and its variants (43) and the interferon (IFN) gene cluster. Thus alterations to this region have a profound impact on cell growth, metabolic activity and signaling. It also contains the lncRNAs *ANRIL*, *p15AS* and now *CAI2*. As *CAI2* is embedded in intron 2 of the *p16/ARF* gene, alterations to this locus will undoubtedly also influence *CAI2* as well. CAI2 was significantly associated with high risk neuroblastoma, a population known to be the least likely to respond to chemotherapy, and a population where the many of patients will relapse and die (18)). Thus CAI2 could play an additional role as a biomarker of advanced stage neuroblastoma, but it is premature to implicate it in response to chemotherapy. Nevertheless, it is clear now that lncRNAs may act not only as biomarkers and/or be prognostically significant, but that their modulation may influence growth and response to therapy. Therefore, one must now also consider the role of *CAI2* when considering how alterations at this locus influence cell behavior. As such, the role *CAI2* plays in diseases where the inactivation p16 and ARF, such as coronary artery disease, are not consistent with the known cell cycle regulatory functions of the proteins, should be considered. Based on this data and the central role this locus plays in multiple human diseases, we believe that *CAI2* must be considered in any future analyses of the genes of this locus on tumorigenesis specifically, and 9p21-associated disease pathogeneses in general.

Sequence has been submitted to Genbank with a Submission ID #1642929**, accession #** KF311101**.**

References:

1. Malecova B, Morris KV. Transcriptional gene silencing through epigenetic changes mediated by non-coding RNAs. Curr Opin Mol Ther. 2010;12:214-22.
2. Ponting CP, Oliver PL, Reik W. Evolution and functions of long noncoding RNAs. Cell. 2009;136:629-41.
3. Mattick JS, Taft RJ, Faulkner GJ. A global view of genomic information--moving beyond the gene and the master regulator. Trends Genet. 2010;26:21-8.
4. Szell M, Bata-Csorgo Z, Kemeny L. The enigmatic world of mRNA-like ncRNAs: their role in human evolution and in human diseases. Semin Cancer Biol. 2008;18:141-8.
5. Ellis BC, Molloy PL, Graham LD. CRNDE: A Long Non-Coding RNA Involved in CanceR, Neurobiology, and DEvelopment. Frontiers in genetics. 2012;3:270.
6. Gupta RA, Shah N, Wang KC, Kim J, Horlings HM, Wong DJ, et al. Long non-coding RNA HOTAIR reprograms chromatin state to promote cancer metastasis. Nature. 2010;464:1071-6.
7. Chisholm KM, Wan Y, Li R, Montgomery KD, Chang HY, West RB. Detection of long non-coding RNA in archival tissue: correlation with polycomb protein expression in primary and metastatic breast carcinoma. PloS one. 2012;7:e47998.
8. Lv XB, Lian GY, Wang HR, Song E, Yao H, Wang MH. Long Noncoding RNA HOTAIR Is a Prognostic Marker for Esophageal Squamous Cell Carcinoma Progression and Survival. PloS one. 2013;8:e63516.
9. Kim K, Jutooru I, Chadalapaka G, Johnson G, Frank J, Burghardt R, et al. HOTAIR is a negative prognostic factor and exhibits pro-oncogenic activity in pancreatic cancer. Oncogene. 2013;32:1616-25.
10. Diccianni MB, Chilcote RR, Yu A. The genes of chromosomes 9p21 (p16, p15, ARF, MTAP) in pediatric acute leukemia: Inactivation and exploitation for tumor-targeted therapeutics. Trends In Cancer Research. 2007;2:135-49.
11. Gil J, Peters G. Regulation of the INK4b-ARF-INK4a tumour suppressor locus: all for one or one for all. Nature reviews Molecular cell biology. 2006;7:667-77.
12. Pasmant E, Sabbagh A, Vidaud M, Bieche I. ANRIL, a long, noncoding RNA, is an unexpected major hotspot in GWAS. FASEB journal : official publication of the Federation of American Societies for Experimental Biology. 2011;25:444-8.
13. Pasmant E, Laurendeau I, Heron D, Vidaud M, Vidaud D, Bieche I. Characterization of a germ-line deletion, including the entire INK4/ARF locus, in a melanoma-neural system tumor family: identification of ANRIL, an antisense noncoding RNA whose expression coclusters with ARF. Cancer research. 2007;67:3963-9.
14. Yu W, Gius D, Onyango P, Muldoon-Jacobs K, Karp J, Feinberg AP, et al. Epigenetic silencing of tumour suppressor gene p15 by its antisense RNA. Nature. 2008;451:202-6.
15. Visel A, Zhu Y, May D, Afzal V, Gong E, Attanasio C, et al. Targeted deletion of the 9p21 non-coding coronary artery disease risk interval in mice. Nature. 2010;464:409-12.
16. Wan G, Mathur R, Hu X, Liu Y, Zhang X, Peng G, et al. Long non-coding RNA ANRIL (CDKN2B-AS) is induced by the ATM-E2F1 signaling pathway. Cellular signalling. 2013;25:1086-95.
17. Bochenek G, Hasler R, El Mokhtari NE, Konig IR, Loos BG, Jepsen S, et al. The large non-coding RNA ANRIL, which is associated with atherosclerosis, periodontitis and several forms of cancer, regulates ADIPOR1, VAMP3 and C11ORF10. Human molecular genetics. 2013;22:4516-27.
18. Yu AL, Gilman AL, Ozkaynak MF, London WB, Kreissman SG, Chen HX, et al. Anti-GD2 antibody with GM-CSF, interleukin-2, and isotretinoin for neuroblastoma. The New England journal of medicine. 2010;363:1324-34.
19. Diccianni MB, Omura-Minamisawa M, Batova A, Le T, Bridgeman L, Yu AL. Frequent deregulation of p16 and the p16/G1 cell cycle-regulatory pathway in neuroblastoma. International journal of cancer Journal international du cancer. 1999;80:145-54.

20. Omura-Minamisawa M, Diccianni MB, Chang RC, Batova A, Bridgeman LJ, Schiff J, et al. p16/p14(ARF) cell cycle regulatory pathways in primary neuroblastoma: p16 expression is associated with advanced stage disease. Clinical cancer research : an official journal of the American Association for Cancer Research. 2001;7:3481-90.
21. Lin YC, Diccianni MB, Kim Y, Lin HH, Lee CH, Lin RJ, et al. Human p16gamma, a novel transcriptional variant of p16(INK4A), coexpresses with p16(INK4A) in cancer cells and inhibits cell-cycle progression. Oncogene. 2007;26:7017-27.
22. Diccianni MB, Chau LS, Batova A, Vu TQ, Yu AL. The p16 and p18 tumor suppressor genes in neuroblastoma: implications for drug resistance. Cancer Letters. 1996;104:183-92.
23. Summerhill EM, Wood K, Fishman MC. Regulation of tyrosine hydroxylase gene expression during differentiation of neuroblastoma cells. Brain research. 1987;2:99-103.
24. Thiele CJ. Neuroblastoma. In: Masters J, editor. Human Cell Culture UK: Kluwer Academic Publishers; 1998. p. 21-35.
25. Lin RJ, Lin YC, Chen J, Kuo HH, Chen YY, Diccianni MB, et al. microRNA signature and expression of Dicer and Drosha can predict prognosis and delineate risk groups in neuroblastoma. Cancer research. 2010;70:7841-50.
26. Chen Y, Stallings RL. Differential Patterns of MicroRNA Expression in Neuroblastoma Are Correlated with Prognosis, Differentiation, and Apoptosis. Cancer research. 2007;67:976-83.
27. Yu M, Ohira M, Li Y, Niizuma H, Oo ML, Zhu Y, et al. High expression of ncRAN, a novel non-coding RNA mapped to chromosome 17q25.1, is associated with poor prognosis in neuroblastoma. International journal of oncology. 2009;34:931-8.
28. Zhu Y, Yu M, Li Z, Kong C, Bi J, Li J, et al. ncRAN, a newly identified long noncoding RNA, enhances human bladder tumor growth, invasion, and survival. Urology. 2011;77:510.e1-5.
29. Castelnuovo M, Massone S, Tasso R, Fiorino G, Gatti M, Robello M, et al. An Alu-like RNA promotes cell differentiation and reduces malignancy of human neuroblastoma cells. FASEB journal : official publication of the Federation of American Societies for Experimental Biology. 2010;24:4033-46.
30. Scaruffi P, Stigliani S, Moretti S, Coco S, De Vecchi C, Valdora F, et al. Transcribed-Ultra Conserved Region expression is associated with outcome in high-risk neuroblastoma. BMC cancer. 2009;9:441.
31. Mestdagh P, Fredlund E, Pattyn F, Rihani A, Van Maerken T, Vermeulen J, et al. An integrative genomics screen uncovers ncRNA T-UCR functions in neuroblastoma tumours. Oncogene. 2010;29:3583-92.
32. Watters KM, Bryan K, Foley NH, Meehan M, Stallings RL. Expressional alterations in functional ultra-conserved non-coding RNAs in response to all-trans retinoic acid--induced differentiation in neuroblastoma cells. BMC cancer. 2013;13:184.
33. Lal A, Kim HH, Abdelmohsen K, Kuwano Y, Pullmann R, Jr., Srikantan S, et al. p16(INK4a) translation suppressed by miR-24. PloS one. 2008;3:e1864.
34. Faghihi MA, Modarresi F, Khalil AM, Wood DE, Sahagan BG, Morgan TE, et al. Expression of a noncoding RNA is elevated in Alzheimer's disease and drives rapid feed-forward regulation of beta-secretase. Nature medicine. 2008;14:723-30.
35. Di Ruscio A, Ebralidze AK, Benoukraf T, Amabile G, Goff LA, Terragni J, et al. DNMT1-interacting RNAs block gene-specific DNA methylation. Nature. 2013;503:371-6.
36. Rinn JL, Kertesz M, Wang JK, Squazzo SL, Xu X, Brugmann SA, et al. Functional demarcation of active and silent chromatin domains in human HOX loci by noncoding RNAs. Cell. 2007;129:1311-23.
37. Mitra SA, Mitra AP, Triche TJ. A central role for long non-coding RNA in cancer. Frontiers in genetics. 2012;3:17.
38. Lee JT. Epigenetic regulation by long noncoding RNAs. Science (New York, NY). 2012;338:1435-9.

39. Zhao Y, Guo Q, Chen J, Hu J, Wang S, Sun Y. Role of long non-coding RNA HULC in cell proliferation, apoptosis and tumor metastasis of gastric cancer: a clinical and in vitro investigation. Oncology reports. 2014;31:358-64.
40. Tsubari M, Tiihonen E, Laiho M. Cloning and characterization of p10, an alternatively spliced form of p15 cyclin-dependent kinase inhibitor. Cancer research. 1997;57:2966-73.
41. Robertson KD, Jones PA. Tissue-specific alternative splicing in the human INK4a/ARF cell cycle regulatory locus. Oncogene. 1999;18:3810-20.
42. Williams RT, Barnhill LM, Kuo HH, Lin WD, Batova A, Yu AL, et al. Chimeras of p14ARF and p16: Functional Hybrids with the Ability to Arrest Growth. PloS one. 2014;9:e88219.
43. Schmid M, Sen M, Rosenbach MD, Carrera CJ, Friedman H, Carson DA. A methylthioadenosine phosphorylase (MTAP) fusion transcript identifies a new gene on chromosome 9p21 that is frequently deleted in cancer. Oncogene. 2000;19:5747-54.

Figure Legends:

Fig 1: The discovery of *CAI2* as a tumor expressed ncRNA. (A) The 5' and 3' RACE smear (RS) and RACE band (RB) cut out of an agarose gel and cloned are boxed. A 100bp molecular weight ladder is included in the 3' RACE figure; **(B)** The fragment of 9p21 containing the genomic orientation of ARF, p16, p16γ and *CAI2* exons and transcripts are illustrated, with the RACE primers and results illustrated. ARF exon 1 (X1β), *p16* exon 1 (X1α), *p16/ARF* exon 2 (X2) and 3 coding (X3) and exon γ (Xγ) are shown; **(C)** The ORFs greater than 40 AA are illustrated relative to the entire *CAI2* transcript. The many ORFs smaller than 40 AA are unlabeled and shaded in grey; **(D)** *CAI2*, ORF2 and p16 were assessed for protein production using the Promega TNT Coupled Reticulocyte Lysate Systems. The luciferase control yielded a sharp band of the correct molecular weight (lane 1). *p16* yielded a faint band at the correct molecular weight of 16 kDa (lane 2), consistent with the paucity of methionine (N=5) and cysteine (N=1) residues. Neither *ORF2* (lane 3) nor *CAI2* in either the sense (lane 4) or antisense (lane 5) orientations yielded any evidence of a protein; **(E)** *CAI2* was detected only in reverse-transcribed RNA. And though *CAI2* sequence could be amplified from genomic DNA, amplification was fully abolished by the same DNAse treatment the RNA samples were subjected to; **(F)** Representative non-quantitative amplifications demonstrate robust expression of *CAI2* in most tumor cell lines (HL60, NB20 and HeLa), though some tumor cell lines (PCL1643) and most normal samples (MNC) express *CAI2* only weakly; Molt4 are deleted (summarized in Supplemental Table 2).

Fig 2: *CAI2*, *p16* and *ARF* expression in normal tissue and after CAI2 transfection. (A) A quantitative PCR analysis of *p16, ARF* and *CAI2* in normal human tissues. SJ-SA-1 (strongly expresses *p16*, *ARF* and *CAI2) and* Be2C/ADR5 (deleted for all three genes) cell lines are included as controls. All expressions are compared to *CAI2* in fibroblasts whose expression is set as 1 for comparison, demonstrating CAI2 expression is very low in most tissues compared to p16 and ARF. **(B)** A Spearman-Rank Correlation (SRC) analysis of *CAI2*, *p16* and *ARF* expression in primary tissue demonstrates the association each gene has with the other; **C)** NMB7 cells were transfected with ps*CAI2* and expression of *CAI2*, p16 and ARF after 48h were compared to cells transfected with a vector containing a scrambled sequence; **D)** The same cultures of transfected cells as in Figure 2C were counted prior to lysing and RNA extraction. The percentage of viable cells after transfection with the control scrambled vector (psSC2) or the *CAI2* expression vector (ps*CAI2)* versus lipid only is shown.

Fig 3: NMB7 cells morphologically change and p16, ARF and CAI2 expression increase with serial passage. (A) NMB7 cells at pre-transformation (shown at passage 10) have a rounded, trapezoid-like morphology; **(B)** After prolonged serial passage (shown at passage 22), cells morphologically change into an elongated structure with long protrusions; **(C)** RNA was extracted from NMB7 during serial passage (P) and *CAI2, p16, ARF* and *TH* expression determined by qRT-PCR; **(D)** Low and high passage (pass) NMB7 cells were cultured for 24h in the presence of complete media (untreated), complete media + 5 μM RA, or media without sera (0% FBS) for 24h before being visually assessed and expression determined. Parallel cultures were also continued for 72h, but loss of viability in the treated low passage cells precluded harvesting of RNA. See also Supplemental Figure S3 and Supplemental Table 3.

Fig 4: CAI2 expression is associated with advanced stage neuroblastoma and age at diagnosis. (A) *CAI2* expression is significantly associated with high risk/advanced stage neuroblastoma (P=0.005, Kruskal-Wallis test, stage 4S, 1 and 2 vs. stage 3 vs. stage 4). MYCN amplified samples are shown as hollow symbols and were not significantly associated with CAI2 expression. For illustration purposes, the single highest *CAI2* expression data point in a stage 4 tumor sample, with a relative expression value of 771, is not shown. A Spearman-Rank Correlation (SRC) analysis of *CAI2* expression vs. stage illustrates the significant trend toward higher CAI2 expression in advanced stage neuroblastoma vs. low stage **(B)** CAI2 expression is significantly associated with age at diagnosis (dx) for all patients ($p<0.002$); and **(C)** for patients diagnosed with advanced stage disease (stage 3 and 4) only ($p<0.05$).

Fig 5: CAI2 expression is an independent prognostic risk factor. *CAI2* expression is plotted versus event-free survival (**A)** or overall survival **(B)** in all neuroblastoma patients where it is significantly associated with survival. It is also plotted versus event-free survival **(C)** and overall survival **(D)** in advanced stage 3 and 4 neuroblastoma patients only where despite its association with advanced stage disease, did not independently associate with outcome in this patient population. Single variable logrank analyses are shown.

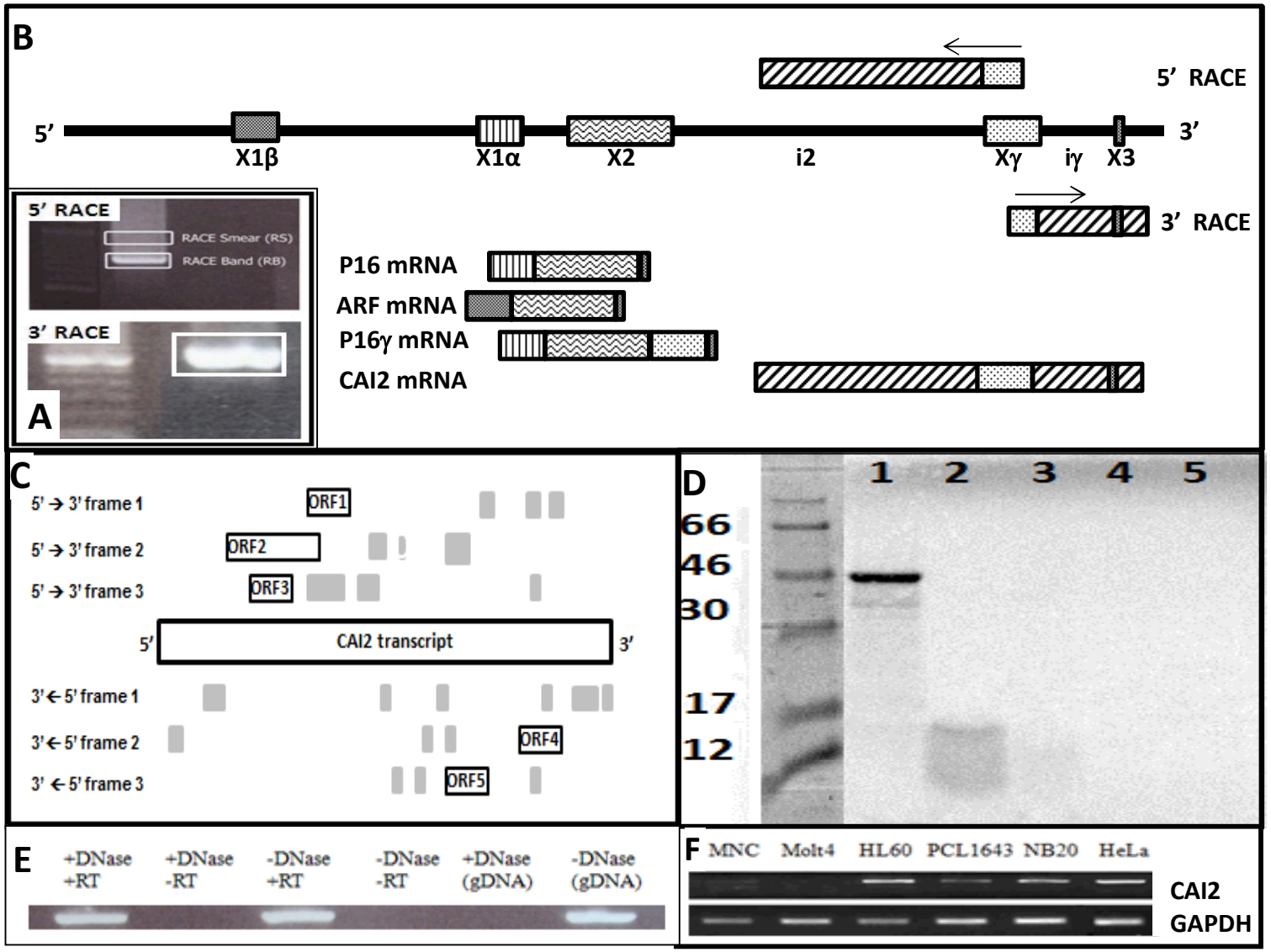
B
5' RACE
5'
3'
X1β
X1α
X2
i2
Xγ
iγ
X3
3' RACE
P16 mRNA
ARF mRNA
P16γ mRNA
CAI2 mRNA
5' RACE
RACE Smear (RS)
RACE Band (RB)
3' RACE
A
C
5' → 3' frame 1
5' → 3' frame 2
5' → 3' frame 3
ORF1
ORF2
ORF3
5'
CAI2 transcript
3'
3' ← 5' frame 1
3' ← 5' frame 2
3' ← 5' frame 3
ORF4
ORF5
D
1 2 3 4 5
66
46
30
17
12
E
+DNase +RT
+DNase -RT
-DNase +RT
-DNase -RT
+DNase (gDNA)
-DNase (gDNA)
F
MNC Molt4 HL60 PCL1643 NB20 HeLa
CAI2
GAPDH

Figure 1

Figure 2

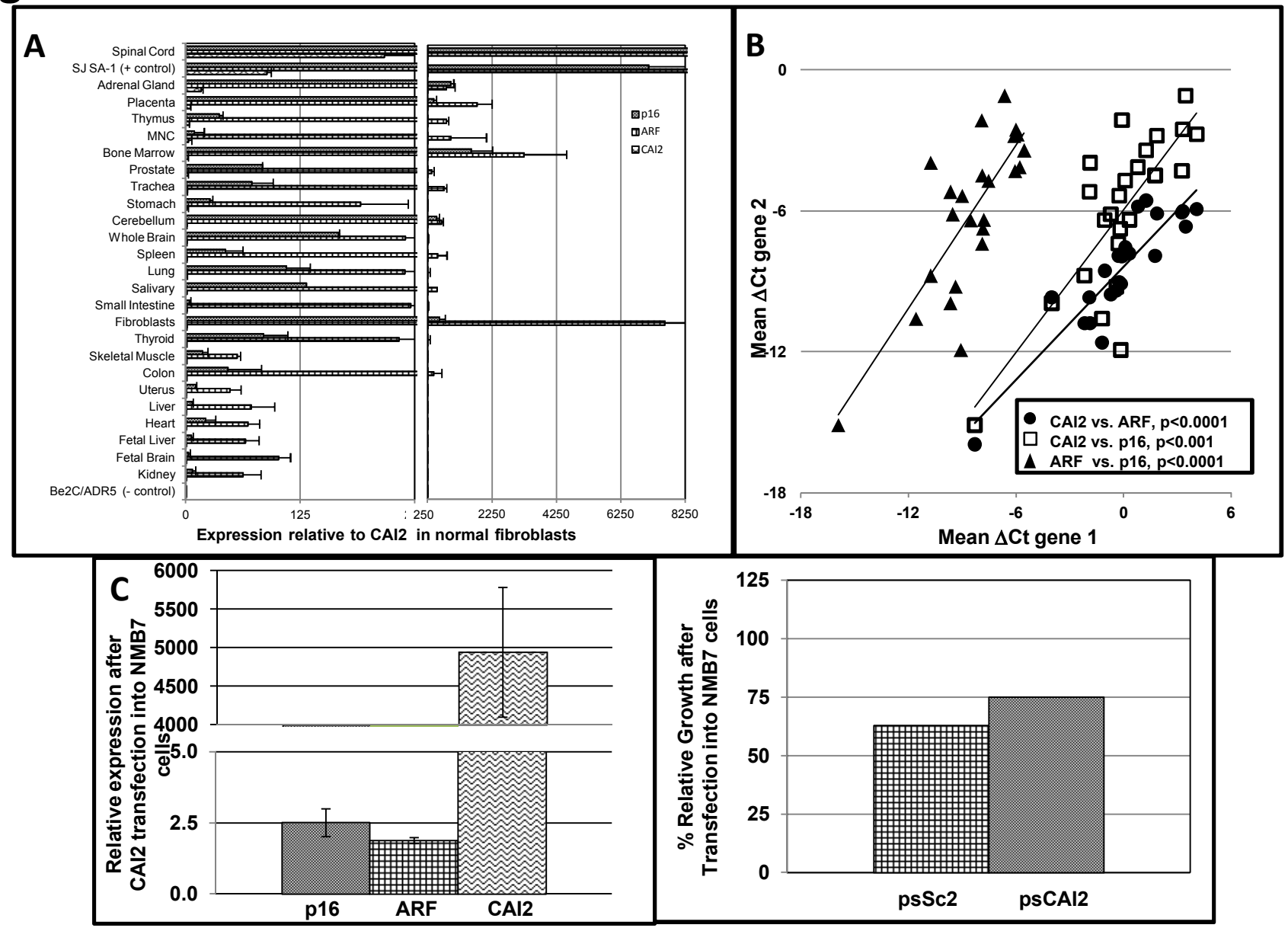
A
Spinal Cord
SJ SA-1 (+ control)
Adrenal Gland
Placenta
Thymus
MNC
Bone Marrow
Prostate
Trachea
Stomach
Cerebellum
Whole Brain
Spleen
Lung
Salivary
Small Intestine
Fibroblasts
Thyroid
Skeletal Muscle
Colon
Uterus
Liver
Heart
Fetal Liver
Fetal Brain
Kidney
Be2C/ADR5 (- control)
p16
ARF
CAI2
0
125
250
2250
4250
6250
8250
Expression relative to CAI2 in normal fibroblasts
B
0
-6
-12
-18
Mean ΔCt gene 2
-18
-12
-6
0
6
Mean ΔCt gene 1
CAI2 vs. ARF, p<0.0001
CAI2 vs. p16, p<0.001
ARF vs. p16, p<0.0001
C
6000
5500
5000
4500
4000
5.0
2.5
0.0
Relative expression after CAI2 transfection into NMB7 cells
p16
ARF
CAI2
125
100
75
50
25
0
% Relative Growth after Transfection into NMB7 cells
psSc2
psCAI2

Figure 3

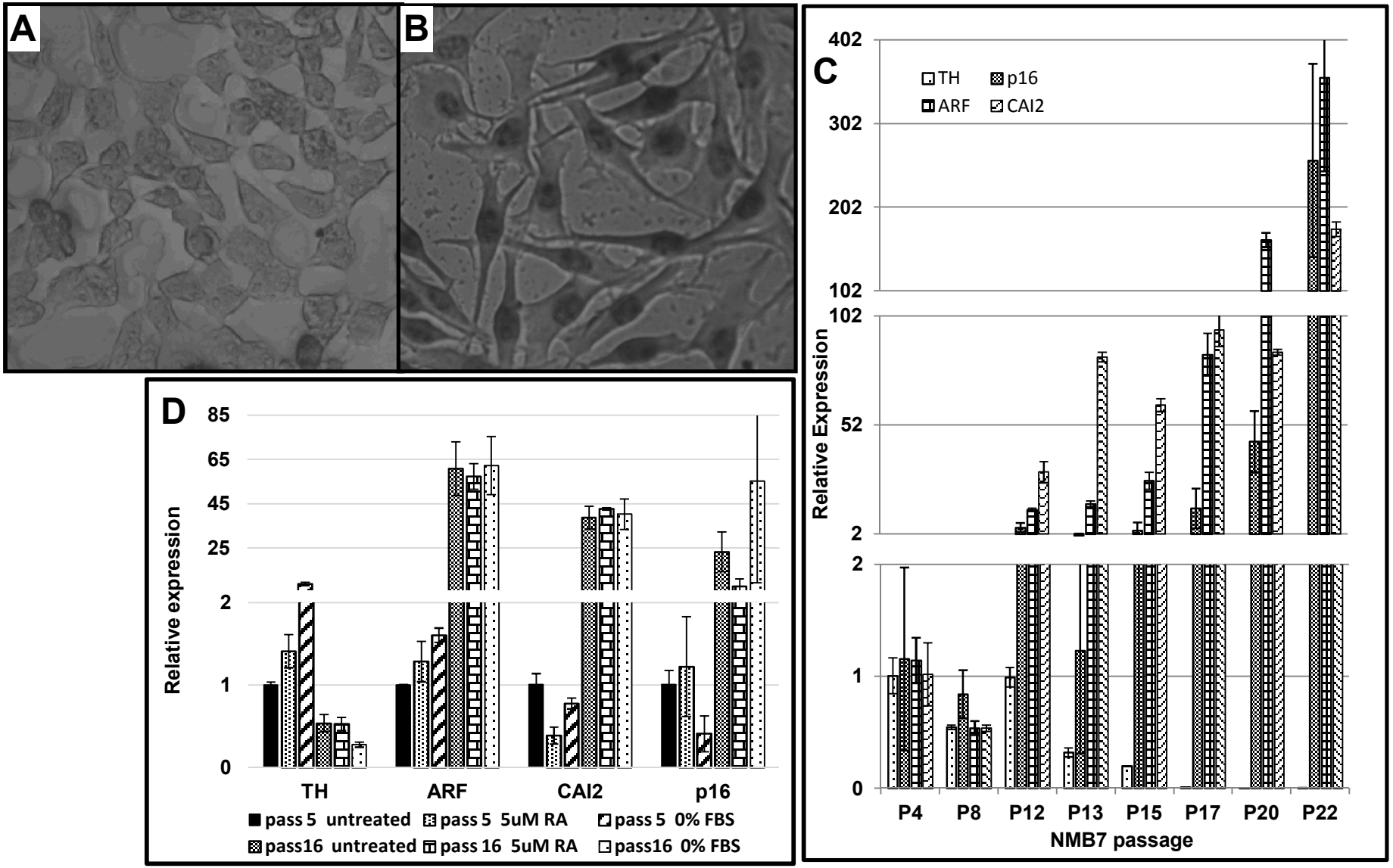
A
B
C
TH
p16
ARF
CAI2
402
302
202
102
102
52
2
2
1
0
Relative Expression
P4
P8
P12
P13
P15
P17
P20
P22
NMB7 passage
D
85
65
45
25
2
1
0
Relative expression
TH
ARF
CAI2
p16
pass 5 untreated
pass 5 5uM RA
pass 5 0% FBS
pass16 untreated
pass 16 5uM RA
pass16 0% FBS

Figure 4

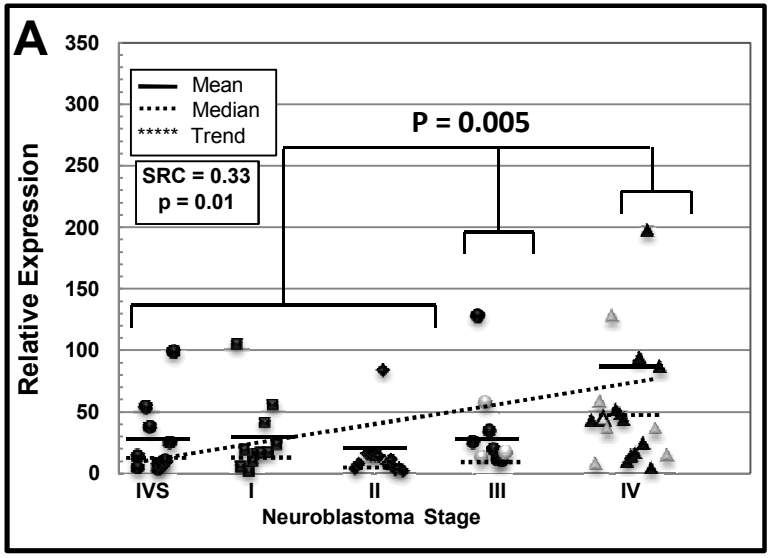
A
Mean
Median
***** Trend
SRC = 0.33
p = 0.01
P = 0.005
Relative Expression
350
300
250
200
150
100
50
0
IVS
I
II
III
IV
Neuroblastoma Stage

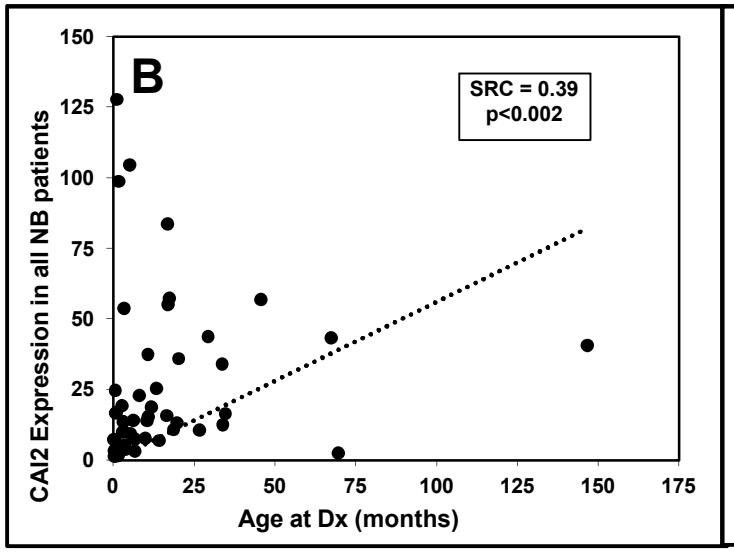
B
SRC = 0.39
p<0.002
CAI2 Expression in all NB patients
150
125
100
75
50
25
0
0
25
50
75
100
125
150
175
Age at Dx (months)

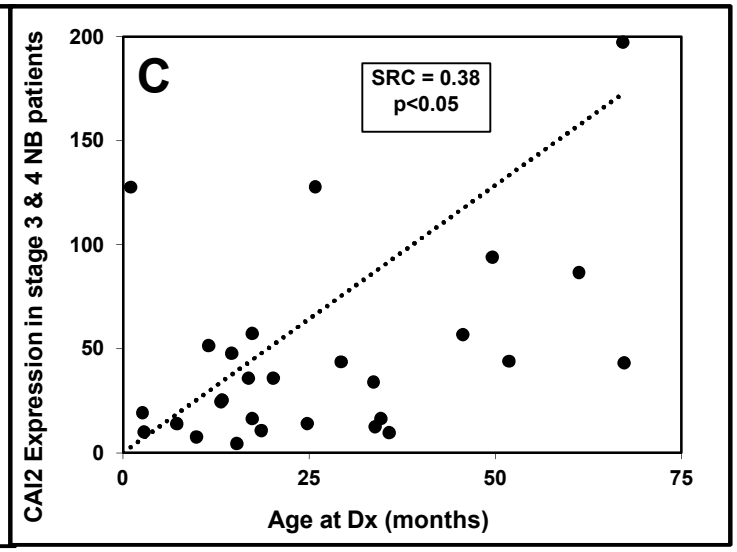
C
SRC = 0.38
p<0.05
CAI2 Expression in stage 3 & 4 NB patients
200
150
100
50
0
0
25
50
75
Age at Dx (months)

Figure 5

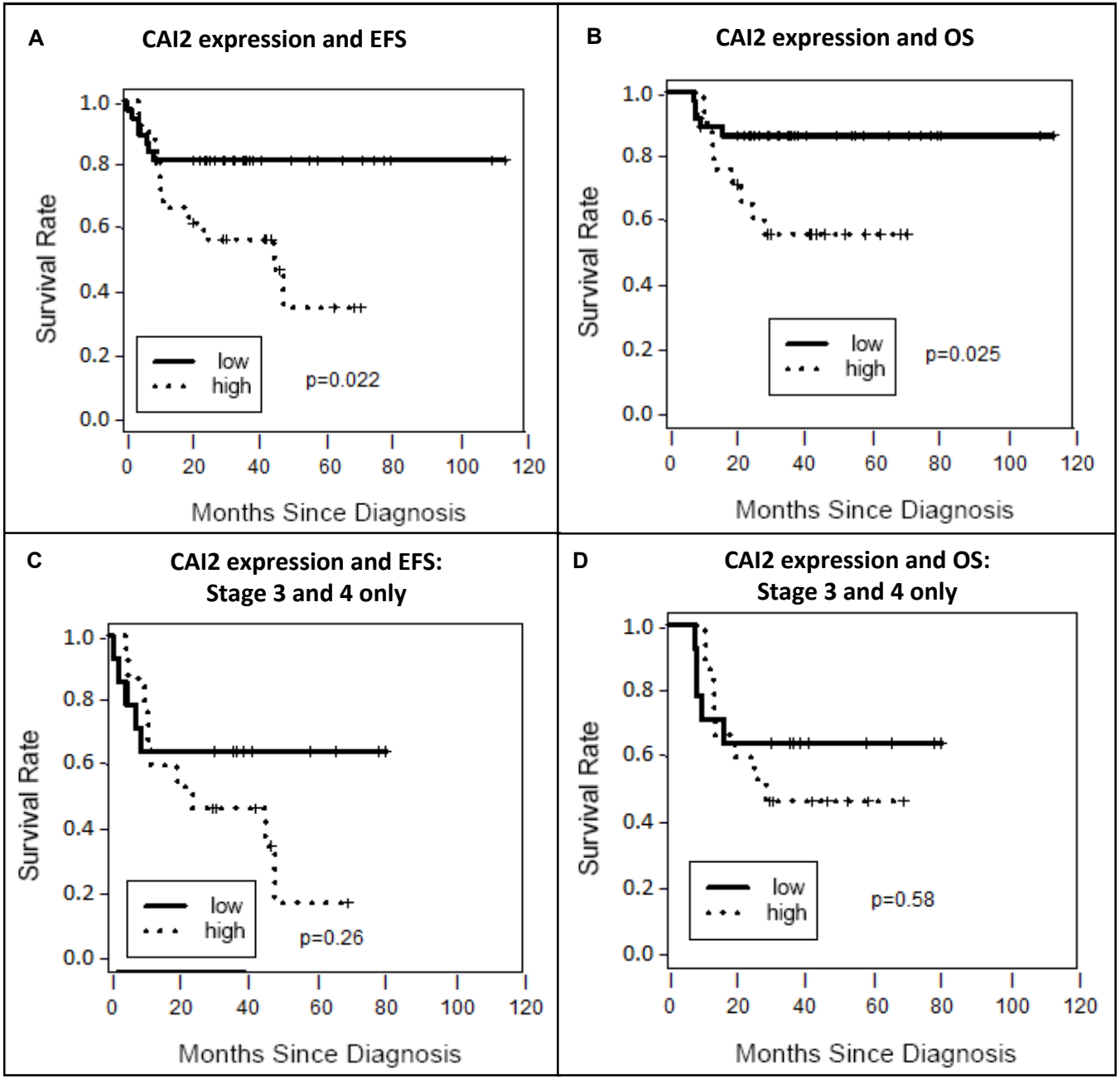
A
CAI2 expression and EFS
Survival Rate
1.0
0.8
0.6
0.4
0.2
0.0
low
high
p=0.022
0
20
40
60
80
100
120
Months Since Diagnosis
B
CAI2 expression and OS
Survival Rate
low
high
p=0.025
Months Since Diagnosis
C
CAI2 expression and EFS:
Stage 3 and 4 only
Survival Rate
low
high
p=0.26
Months Since Diagnosis
D
CAI2 expression and OS:
Stage 3 and 4 only
Survival Rate
low
high
p=0.58
Months Since Diagnosis